Plasma perturbation induced by laser photodetachment

M. Nishiura and M. Sasao
National Institute for Fusion Science, 322-6 Oroshi, Toki, Gifu 509-5292, Japan

M. Wada
Doshisha University, Kyotanabe, Kyoto 610-0321, Japan

M. Bacal
Laboratoire de Physique des Milieux Ionises, U.M.R. 7648 du C.N.R.S., Ecole Polytechnique, 91128 Palaiseau, France
(Received 17 July 2000; published 27 February 2001)

The plasma dynamics arising from laser photodetachment is discussed herein theoretically and experimentally. The hybrid fluid-kinetic model, where the positive ions and electrons are treated by the fluid theory and the negative ions are treated within the ballistic approximation, is extended and applied to the analysis of densities perturbed by laser photodetachment. The agreement between the theory and measured data confirms the validity of the considered plasma dynamics model. This model, including the positive ion perturbation, shows a good agreement with the time evolution and the spatial distribution of perturbed electron densities which are measured by a Langmuir probe inside and outside the laser beam. From the overshoot in the time evolution of perturbed electron current in the center of the laser beam, the positive ion temperature was found to be in the range 0.1–0.25 eV, while the electron temperature changes from 0.3 to 3.2 eV.

DOI: 10.1103/PhysRevE.63.036408 PACS number(s): 52.38.−r, 51.10.+y, 51.50.+v, 52.70.−m

I. INTRODUCTION

Plasma, which contains negative ions, has been studied in fields such as astrophysics, negative ion source development, and divertor plasma physics for nuclear fusion research. For a better understanding of production mechanisms of negative ions, the laser photodetachment method assisted by a Langmuir probe is a most useful diagnostic tool for negative ions in plasma. We can obtain information on negative ion density and temperature and optimize the plasma characteristics using these data.

A laser of photon energy higher than the electron affinity causes the laser photodetachment such as $A^- + h\nu \rightarrow A + e^-$. This reaction leads to a sudden increase of the electron density, δn_e, on the laser path in plasmas containing negative ions. When all the negative ions are destroyed, $\delta n_e / n_e$ corresponds to the ratio of the negative ion density to the electron density, n_- / n_e. Using this relation, negative ion densities of hydrogen in plasma were first measured by the use of laser photodetachment assisted with a positively biased Langmuir probe in 1979 [1,2]. The time evolution of electron current after photodetachment showed a slow recovery on the time scale of positive or negative ion transit time. A typical feature of the photodetachment signal is the presence of an overshoot after the initial pulse of the electron current and before this current recovers its initial value [3,4].

Two methods have been proposed for the determination of the negative ion temperature. Devynck *et al.* [3] measured the negative ion temperature from the recovery time of the electron density. Stern *et al.* [4] proposed and used the two laser photodetachment method for determining the negative ion temperature. The consistency of these two methods was verified experimentally. Devynck *et al.* [3] and Stern *et al.* [4] have reported that the velocity of outgoing electrons is roughly equal to the thermal velocity of negative ions. In order to explain this phenomenon, the kinetic equation coupled with the Poisson's equation has been utilized, neglecting the electric field dependent terms [4]. Stern *et al.* [4] have developed the theory of transport dynamics in which local neutrality is preserved in the laser irradiated region due to ''monopolar drift'' (particles with the same charge are counterflowing, this is in contrast with the well-known ambipolar drift that involves oppositely charged species flowing in the same direction). The analytical solution of the flow of negative ions toward the laser axis is given by $n_-(r=0,t) = n_{-0} \exp[-(R/v_{\mathrm{th}}^- t)^2]$, where r is the distance from the center of the laser beam, R is the laser radius, v_{th}^- is the thermal velocity of negative ions, and n_{-0} is the background negative ion density. From this result the recovery time of excess electron current τ_r is inversely proportional to the thermal velocity of negative ions: $\tau_r \propto R/v_{\mathrm{th}}^-$. This ballistic model is valid only for the early stage of the negative ion recovery and for small potential perturbation. The overshoot in the time evolution of excess electron current after photodetachment could not be explained within this theory.

The ballistic model was extended to include the effects of the self-consistent electric field [5]. Friedland, Ciubotariu, and Bacal [5] have proposed the theory of the hybrid fluid-kinetic model in which the motion of electrons and positive ions obey the fluid equation and that of negative ions is governed by the kinetic equation. The general formulations for negative ion density $n_-(r,t)$ and photodetached electron density $\delta n_e(r,t)$ are given in Ref. [5]. For actual applications, $n_-(r=0,t)$ and $\delta n_e(r,t)$ are demonstrated using the smoothing functions for both slab and cylindrical geometry instead of a delta function. The time variation of photodetached electron current including an overshoot at $r=0$ is calculated in Ref. [5]. It is found that the ratio of the amplitude of the overshoot current to the photodetached electron

depends on the ratio of electron temperature to positive ion temperature, T_e/T_+. Friedland, Ciubotariu, and Bacal concluded that the depletion of positive ions, arising from the difference in the thermal velocities of electrons and ions, causes the overshoot current. Nishiura, Sasao, and Bacal [6] applied the hybrid fluid-kinetic model to the analysis of the dependence on T_e of the measured photodetachment-current to overshoot-current ratios versus time assuming a reasonable T_+ [6]. These authors have also shown that the amplitude of photodetachment currents is independent of laser photon energies used for photodetachment. These results show that the theoretical model and the relation of $n_-/n_e = \delta n_e/n_e$ are valid.

Ivanov *et al.* [7] pointed out the importance for the negative ion recovery of the self-consistent electric field in the case of negative ion to positive ion density ratio higher than 0.1. As another approach, they have also studied the dynamics of perturbed electrons in a planar geometry under the conditions that $T_+ \sim T_e$ using the linearized Vlasov equation [8]. The solution for perturbed electrons coincided with the one obtained by the hybrid fluid-kinetic model in the limit $T_+ \to 0$.

These models are compared with the experimental results that are measured inside the laser beam. As the density perturbation should propagate into the plasma region outside the laser beam, the complete analysis of the perturbed density profile including the region $r > R$ can be a good confirmation of the validity of theoretical models. Thus the change of electron density in both time and space due to photodetachment in a cylindrical geometry is analyzed in this paper. We begin with introducing the hybrid fluid-kinetic model and extend it to analyze the plasma response using the general solutions of $\delta n_e(r,t)$ and $\delta n_-(r,t)$ until the plasma recovers to the original condition. The results are compared with the experimental data of the corresponding condition in order to confirm the hybrid fluid-kinetic model.

II. BASIC EQUATION AND MODEL

Hydrogen plasmas in negative ion sources usually contain various species: positive ions (H^+, H_2^+, H_3^+), negative ions (H^-), and electrons. The plasma considered here is assumed to consist of only three species of charged particles: positive ions (H_3^+), electrons (e^-), and negative ions (H^-). The magnetic field can be ignored and the plasma is homogeneous in our case. When the plasma is irradiated with a laser beam, which destroys all the negative ions in its path, $r ? R$, the electron density increases suddenly due to the photodetachment reaction in the laser irradiated region. For $r > R$, all the species are not perturbed by photodetachment at $t = 0$. The excess electrons in the laser irradiated region, $r ? R$, do not feel anything initially, but the density gradient influences the electrons near the edge ($r \sim R$). The negative ions fill the depleted region across the discontinuous edge. At the same time, excess electrons and positive ions move outward in order to compensate the total charge balance. Finally the perturbed plasma recovers to the initial condition on the time scale of $R/v_{\rm th}^-$.

The negative ion production during the plasma response is negligible compared to the negative ion flux entering into the laser illuminated region due to monopolar drift. The following rate equation for the total negative ion density N_- in the cylindrical volume illuminated by the laser around the probe of length L can be used to compare these two negative ion fluxes, although the collisional part of it is not justified since the mean free path of electrons is longer than the laser radius:

$$\frac{dN_-}{dt} = 2\pi RL\left[\frac{R}{2}[n_e + \Delta n_e] n(H_{2,v''=5-10}) \overline{\sigma v}(\mathrm{DA}) + n_{-0} v_{\rm th}^-\right]. \quad (1)$$

We use a typical rate coefficient for dissociative attachment calculated by Berlemont, Skinner, and Bacal [9] in hydrogen multicusp discharges. With the initial background electron density $n_{e0} = 10^{10}\,\mathrm{cm}^{-3}$, the background negative hydrogen ion density $n_{-0} = 10^9\,\mathrm{cm}^{-3}$, the density of vibrationally excited molecules in states v'' equal 5–10, $n(H_{2,v''=5-10}) = 5 \times 10^{10}\,\mathrm{cm}^{-3}$, and the rate coefficient [9] for dissociative electron attachment to these molecules $\overline{\sigma v}(\mathrm{DA}) = 4 \times 10^{-9}\,\mathrm{cm}^{-3}/\mathrm{s}$, we find that the flux due to the monopolar drift is a factor of 10^4 larger than the flux due to electron-molecule collisions. This means that we can use a collisionless scheme for plasma particles on the time scale less than a few times of that of recovery.

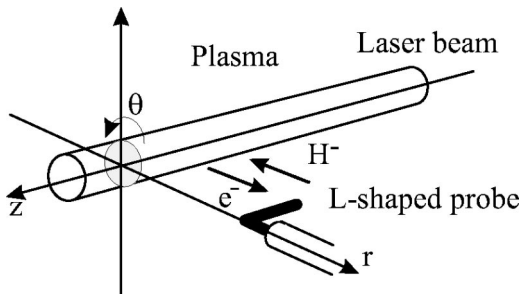

FIG. 1. Illustration of the laser beam and probe position for a model calculation.

The experimental arrangements are shown in Fig. 1. The cylindrical geometry is employed for its analytical advantages. The z direction coincides with the laser axis. The radial direction of the laser is chosen as r. The rotational direction is θ. The cylindrical probe is moved in the radial direction.

With the foregoing in mind, the analytical model of Friedland, Ciubotariu, and Bacal [5] is extended to describe the plasma response caused by photodetachment both inside and outside the laser beam. In the case of cold plasmas, the continuity and momentum equations for positive ions become

$$\frac{\partial(\delta n_+)}{\partial t} + n_0^+ \frac{\partial \delta v^+}{\partial r} = 0, \quad (2)$$

$$M_+ \frac{\partial(\delta v^+)}{\partial t} = -e\frac{\partial(\delta\phi)}{\partial r} - \frac{\gamma_i k_B T^+}{n_0^+}\frac{\partial(\delta n^+)}{\partial r}, \quad (3)$$

where M_+ indicates the mass of the positive ion, k_B the Boltzmann constant, v the velocity of the particle, $\delta\phi$ the perturbed potential, γ_i the adiabatic index for ions ($\gamma_i=3$), δ the perturbed quantity, the subscripts e, $-$, and $+$ the species of charged particles, and the subscript 0 the background density, respectively.

When the bulk and detached electrons are described by a Maxwellian distribution function, the field dependent electron density δn_e is linearized by the Boltzmann relation,

$$\delta n_e = n_{e0}\frac{e(\delta\phi)}{k_B T_e}, \tag{4}$$

where n_{e0} is the background electron density and T_e the electron temperature, respectively. The quasi-neutrality becomes a good approximation in first order,

$$\delta n_+ = n_- - n_{-0} + n_e. \tag{5}$$

The motion of negative ions is described by the kinetic equation:

$$\frac{\partial f^-}{\partial t} + \mathbf{v}\cdot\frac{\partial f^-}{\partial \mathbf{r}} + \frac{e}{M_-}\left(\mathbf{E}+\frac{\mathbf{v}\times\mathbf{B}}{c}\right)\cdot\frac{\partial f^-}{\partial \mathbf{v}} = 0, \tag{6}$$

where f^- indicates the distribution function for negative ions. Since the nonlinear term would be negligible during the early time period and $\mathbf{B}=0$ in an unmagnetized plasma, Eq. (6) can be reduced to the simplified form

$$\frac{\partial f^-}{\partial t} + v\cdot\frac{\partial f^-}{\partial r} = 0. \tag{7}$$

The variation of the negative ion density is given by

$$\Delta n_- \equiv n_- - n_{-0} = \int (f^- - f_0^-)d^3v, \tag{8}$$

with the initial distribution for negative ions, f_0^-.

Here we introduce a Laplace transform in time and a Fourier transform in space with respect to the set of equations (2)–(5), (7), and (8) in order to obtain $\delta\phi(k,\omega)$. The solution for the potential, $\delta\phi(r,t)$, is obtained by inverting the Laplace transform and the Fourier transform. The details of the calculations are similar to those in Ref. [5]. Assuming the ion acoustic velocity, C_s, as comparable to the thermal velocity of negative ions, where $v_{\rm th}^- = (8k_BT_-/\pi M_-)^{1/2}$, as was done by Friedland, the final results for δn_e and δn_- are as follows. For electrons:

$$\frac{\delta n_e(r,t)}{n_{-0}} = 2\int_0^{+\infty}\frac{[v_a^2-(v_{\rm th}^+)^2]\Psi(r,v_at)-[v^2-(v_{\rm th}^+)^2]\Psi(r,vt)}{(\pi^{1/2}v_{\rm th}^-)[v_a^2-v^2]} \times e^{-(v/v_{\rm th}^-)^2}dv. \tag{9}$$

For negative ions:

$$\frac{\delta n_-(r,t)}{n_{-0}} = -\frac{2}{(\pi^{1/2}v_{\rm th}^-)}\int_0^{+\infty}\Psi(r,vt)e^{-(v/v_{\rm th}^-)^2}dv. \tag{10}$$

The mentioned assumption is reasonable because the ion acoustic velocity for H_3^+ is very close to $v_{\rm th}^-$ from the experimental results [6].

The function $\Psi(r,vt)$ in Eqs. (9) and (10), which includes the integration of the Bessel function, takes the following form,

$$\Psi(r,vt) = \int_0^\infty r'dr'\int_0^\infty kdk\left[\frac{\Delta(r')}{n_{-0}}\right] \times\cos(kvt)\cdot J_0(kr)J_0(kr'), \tag{11}$$

where

$$\frac{\Delta(r')}{n_{-0}} = \begin{cases} 1 & \text{if } |r'|\leq R \\ 0 & \text{if } |r'|>R. \end{cases} \tag{12}$$

The step function $\Delta(r')$ is used to represent the initial distribution of excess electrons. This form generally depends on the profile of the laser beam, but it is reasonable to use Eq. (12) for our conditions because we cut the tail of a Gaussian beam to make the boundary of the laser beam sharp. In order to proceed to the integration, Eq. (11) is transformed into

$$\Psi(r,vt) = \int_0^\infty R\cos(kvt)J_0(kr)J_1(kR)dk, \tag{13}$$

with J_0 and J_1 being the Bessel function of the first kind of the order 0 and the order 1. Friedland Ciubotariu, and Bacal [5] provided the function $\Psi(r=0,vt)$ with the help of a smoothing function corresponding to the step function, instead of Eq. (13). Substituting the function $\Psi(r,vt)$ of Eq. (13) into Eq. (10), the integration over v can be carried out [10], and then,

$$\frac{\delta n_-(r,t)}{n_{-0}} = -\frac{2}{(\pi^{1/2}v_{\rm th}^-)}\int_0^{+\infty}J_0(kr)J_1(kR)e^{-(ktv_{\rm th}^-/2)^2}d(kR). \tag{14}$$

Equation (14) at $r=0$ corresponds to Eq. (12) in Ref. [4].

For the sake of convenience and simplicity we introduce dimensionless quantities:

$$x = v/v_{\rm th}^-;\quad \tau = v_{\rm th}^- t/R;\quad \alpha = \sqrt{\gamma_i T_+/T_e};\quad \eta = r/R;\quad \xi = kR. \tag{15}$$

The quantities x and τ may be thought of as the velocity of charged particles in a plasma and the time after the photodetachment occurred, respectively. α denotes the ratio of positive ion temperature to electron temperature. η is the normalized distance from the axis of the laser beam in the radial direction in cylindrical coordinates.

Using these quantities, Eq. (9) for the perturbation of the electron density becomes

$$\frac{\delta n_e(\eta,\tau)}{n_{-0}} = \frac{2}{\sqrt{\pi}} \int_0^{+\infty} \frac{\Psi(\eta,\sqrt{1+\alpha^2}\tau) - (x^2-\alpha^2)\Psi(\eta,x\tau)}{1+\alpha^2-x^2} \times e^{-x^2} dx, \tag{16}$$

where

$$\Psi(\eta,x\tau) = \int_0^{\infty} \cos(x\tau\xi) J_0(\eta\xi) J_1(\xi) d\xi. \tag{17}$$

Equation (10) for the negative ion density becomes

$$\frac{\delta_-(\eta,\tau)}{n_{-0}} = \int_0^{+\infty} J_0(\eta\xi) J_1(\xi) e^{-(\tau\xi/2)^2} d\xi. \tag{18}$$

The integrals in Eqs. (16) and (18) are calculated numerically.

III. EXPERIMENTAL CONFIGURATION

A magnetic multicusp discharge is produced in a stainless-steel vessel 270 mm in length and 210 mm in diameter. Ten rows of ferrite magnets are attached on the cylindrical wall for the plasma confinement. Each end flange of the vessel has also four magnets. The vessel is connected to the ground and serves as an anode. The hydrogen plasma is produced by electrons emitted from two tungsten filaments and accelerated by the discharge voltage.

The L-shaped Langmuir probe is installed in the plasma. The probe tip is made of a tungsten wire 10 mm in length and 0.35 mm in diameter. The probe is positioned by a micrometric screw and can be moved 10 mm along the radial direction. The micrometric screw gives us the positioning precision of 0.25 mm in the radial direction.

A pulsed Nd-yttrium-aluminum-garnet laser was used for photodetachment. The laser beam diameter is limited to 4 mm using an aperture. The laser power is kept constant in the saturation region to detect the excess electron current due to photodetachment. The change of probe current due to photodetachment is detected by a storage scope. The schematic diagrams of the experimental setup and measurement system are shown in Ref. [6].

We verified that the produced dc plasma was uniform and unmagnetized in the central region of the vessel. Plasma parameters of $n_e = 10^{10}-10^{11}\,\mathrm{cm}^{-3}$, $T_e = 0.5-3$ eV, and $n_-/n_e \sim 0.05$ are obtained from the probe $I-V$ characteristics and photodetachment measurement. The relation [1] $n_-/n_e = \Delta I/I_{\mathrm{dc}}$ is used to determine the n_-/n_e ratio because the laser power is high enough to detach all the electrons from H^- ions. The differences between the probe signals measured inside and outside the laser beam are studied in the subsequent sections.

IV. RESULTS AND DISCUSSION

A. The perturbed potential at $\eta = 0$

Figure 2 shows the time evolution of typical probe signals and calculated signals after photodetachment at $\eta = 0$ in the cases of (a) $T_e = 0.86$ eV and (b) $T_e = 0.55$ eV. The hydrogen gas pressure P_g is adjusted to change the electron temperature keeping the discharge current constant. The ordinate indicates the perturbed electron density normalized by the maximum. The abscissa is the time normalized to the recovery time, which is defined as the time when the negative ion density reaches again the initial value. Two experimental traces of δn_e are shown in Figs. 2(a) and 2(b). They are in good agreement with those calculated with $\alpha = 0.59$ in Fig. 2(a) and $\alpha = 0.75$ in Fig. 2(b). As α decreases, the amplitude of the overshoot becomes larger due to the difference of mobility between electrons and positive ions. For longer time τ, the observed photodetachment current approaches zero with a slow oscillation similar to the calculated δn_e.

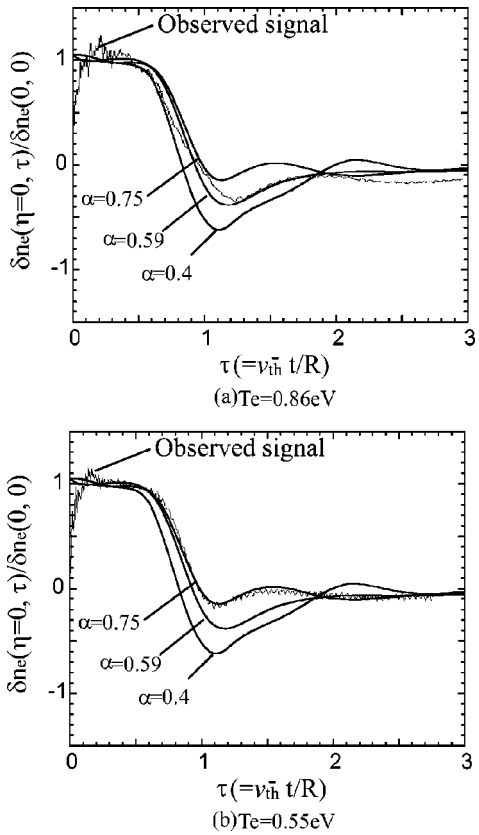

FIG. 2. The observed signal and the calculated traces at $\eta = 0$ (laser beam axis). The photodetachment signal is measured under the conditions: $P_g = 2.2$ mTorr, $V_d = 100$ V, and $I_d = 1$ A in the cases (a) $T_e = 0.86$ eV and (b) $T_e = 0.55$ eV.

The observed δn_e has a slow rise time after photodetachment. This time lag is about 20 ns, which is much larger than the plasma oscillation time (<1 ns) and the pulse duration of the laser ($=5.5$ ns). The time scale is considered to be the propagation time of the perturbed electrons through the probe sheath with an ion acoustic velocity

$$\lambda_D/C_s = \lambda_D/(R/t_r) = 0.1\times10^{-3}/(2\times10^{-3}/400\times10^{-9}) = 20\,\mathrm{ns}.$$

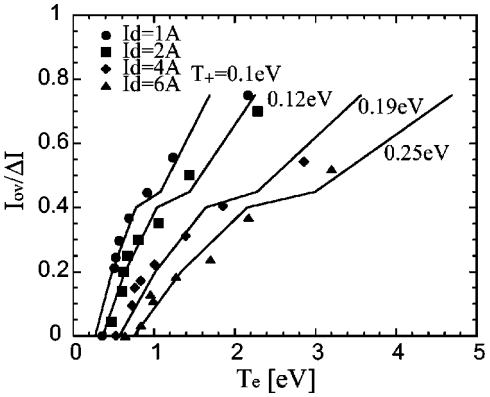

FIG. 3. Dependence of the overshoot signal on the electron temperature for various discharge currents of 1, 2, 4, and 6 A. The symbols indicate the measured data. The four lines indicate the calculated values of the overshoot signal and are fit to coincide with the measured data using the parameter T_+. The electron temperatures were changed by the adjustment of the hydrogen gas pressure.

This information is important and useful for the analysis of sheath formation. However, additional explanations about the rise time are required because the time lag tends to be inversely proportional to the ion acoustic velocity, but independent of the Debye length.

The measured overshoot-current to photodetachment-current ratios $I_{ov}/\Delta I$ versus electron temperature for various discharge currents are plotted in Fig. 3. The photodetachment current with the ratios of $\alpha=0.75$, 0.59, 0.5, and 0.4 is calculated with T_+ as a parameter. The hydrogen gas pressure is adjusted to change the electron temperature. When the discharge current is kept constant, the measured $I_{ov}/\Delta I$ coincides with the corresponding calculated line. The positive ion temperature can be determined using these results. Even if T_e is varied over the range of 0.5–2.5 eV, T_+ with a constant discharge current does not change. This result is reasonable because the positive ions are produced by collisions between high-energy electrons and hydrogen molecules and the electron temperature does not affect the energy of the positive ions formed.

B. Propagation of perturbed potential

Devynck *et al.* [3] and Nishiura Sasao, and Bacal [6] have already reported the outward propagation velocity of the perturbed potential observed experimentally and compared it with the ion acoustic velocity. We confirmed that the peak of perturbed potential moves outward with the ion acoustic velocity and it is not attenuated as a ballistic locus corresponding to $1/r$. For the determination of the effective laser radius, the time evolutions of the perturbed electron density $\delta n_e(\eta,\tau)$ are shown in Fig. 4. The Langmuir probe is located at (a) $r=4$ mm, (b) $r=5$ mm, and (c) $r=6$ mm, respectively. The ordinate indicates the perturbed electron density normalized to that at $r=0$. Although the actual laser beam radius should be 2.0 mm, r is normalized to $R=2.5$ mm because of the density gradient at the laser boundary. The calculated potentials at $\eta=1.6$, 2, and 2.4 are also plotted in Fig. 4. The calculated peaks of perturbed electron

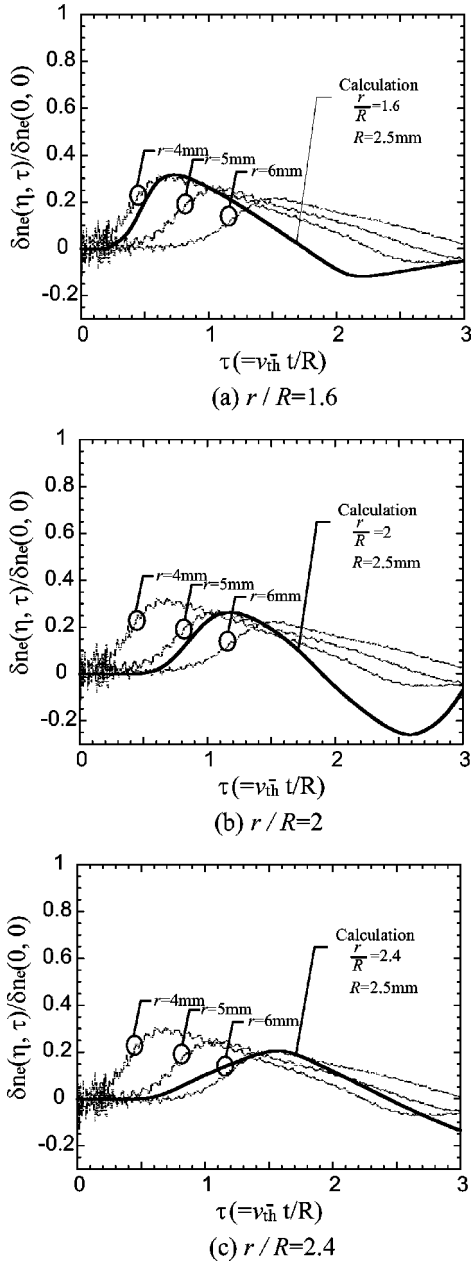

FIG. 4. Comparison between the observed signals and the calculated traces (thick line) under the conditions that $\alpha=0.59$ and $R=2.5$ mm. (a) $r/R=1.6$, (b) 2.0, and (c) 2.4. Experimental data are obtained under the conditions where $n_-/n_e=0.01$, $n_e=7\times10^{10}\,\mathrm{cm}^{-3}$, and $T_e=0.86$ eV in a hydrogen plasma. The peak position of the observed signal agrees with the calculations at each probe position.

density coincide with the observed peaks in each case. However, at a larger time than that of the peak, there is a discrepancy in electron density. The profile of the laser beam may cause the difference in signal width between the observed data and the calculation. The precision of the Langmuir probe would be poor in space to an extent of several Debye lengths.

The perturbed negative ion density is shown in Fig. 5 using Eq. (18) from $\tau=0$ to 3.0. The time scale of the thermal velocity of negative ions governs the recovery time. The

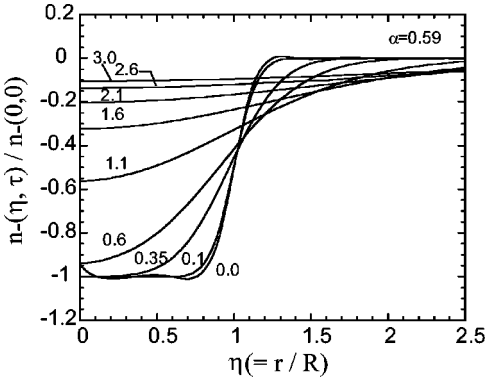

FIG. 5. Calculations of spatial-temporal transition of perturbed densities for negative ions after laser photodetachment.

region depleted in negative ions inside the laser channel is filled with the negative ions gradually from the boundary of the laser path. The recovery of the negative ion density does not depend on α in this approximation. The effect on α should be treated if the positive ion temperature is relatively high.

C. Determination of negative ion density from a signal measured at $\eta \neq 0$

A peak of the perturbed electron density propagates outwardly with the ion acoustic velocity, while its maximum $\delta n_{e\,\max}/\delta n_e(0,0)$ drops inversely proportional to the distance from the center of the laser beam. The maximum of the electron current at each distance is compared with the calculated curves of $\alpha=0$, 0.59, and 0.75 in Fig. 6. Experimental data of $\delta n_{e\,\max}/\delta n_e(0,0)$ agree well with the results of the calculations with $\alpha=0.59$. When α increases, the theoretical values of $\delta n_{e\,\max}/\delta n_e(0,0)$ show a decrease, but not a drastic change. Since the propagation of $\delta n_{e\,\max}/\delta n_e(0,0)$ depends on the ratio of T_e/T_+, a calculation is required to determine n_{-0} from the measured data at $\eta>0$. Even if T_e/T_+ cannot be obtained from the analysis of the signal at $\eta=0$, it is found that $\delta n_e(0,0)$ can be estimated roughly using $\delta n_{e\,\max}$ measured at any distance and using a reasonable value of T_e/T_+. This enables us to determine the negative ion density at $\eta=0$ from the measurement of a perturbed electron density at $\eta>0$.

In terms of physical aspects, the plasma dynamics after photodetachment is considered as follows. In the case of low α, due to the increase of T_e, the positive ion density decreases inside the laser irradiated region and causes the overshoot because of the self-consistent electric field induced by electrons. Then, the electrons are pushed outwardly more as α decreases. In the case of high α, however, the positive ions remain inside the laser-irradiated region, which leads to the decrease of the overshoot.

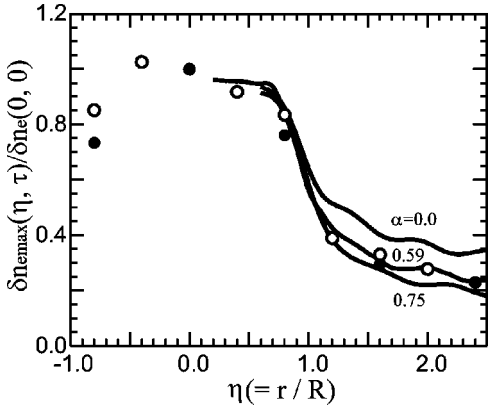

FIG. 6. Change of maximum perturbed electron density versus probe position. The symbols indicate the observed peak value of the probe signal. The data are obtained by moving the probe position with increasing η (open circles) and with decreasing η (closed circles). The thick line is the calculated variation of perturbed electron densities in the case of $\alpha=0$, 0.59, and 0.75 and $R=2.5$ mm.

V. CONCLUSIONS

The time evolution of the electron current induced by the laser photodetachment was measured to verify the hybrid fluid kinetic model inside as well as outside the laser beam. Then we treated the plasma perturbation under the low negative density conditions, where n_-/n_e is less than a few percent, in uniform, collisionless, and unmagnetized hydrogen plasmas. The information about the plasmas inside the laser beam gives us the critical information not only on the negative ion density and temperature, but also on the positive ion temperature. From the measured data outside the laser beam, the negative ion density is estimated numerically using this model. In both cases, the consistency between data inside and outside the laser beam indicates that the electrostatic probe does not influence the plasmas under the conditions of our experiment. It is also clear that the good agreement with measured data shows the validity of this model.

The analysis outside the laser beam would be an effective method under the severe conditions where an electrostatic probe suffers from the laser irradiation. Another method for determining the plasma parameters could make use of the dynamics of the perturbed potential. In future work we will construct a new model with relatively high n_-/n_e and magnetic field.

ACKNOWLEDGMENTS

We would like to thank Professor M. Fujiwara at the National Institute for Fusion Science and Professor T. Kuroda at Chubu University for their encouragement throughout this work. Finally, the present work has been carried out under the Collaboration Research Program at NIFS.

[1] M. Bacal and G. W. Hamilton, Phys. Rev. Lett. **42**, 1538 (1979).

[2] M. Bacal, G. W. Hamilton, A. M. Bruneteau, and H. J. Doucet, Rev. Sci. Instrum. **50**, 719 (1979).

[3] P. Devynck, J. Auvray, M. Bacal, P. Berlemont, J. Bruneteau, R. Leroy, and R. A. Stern, Rev. Sci. Instrum. **60**, 2873 (1989).

[4] R. A. Stern, P. Devynck, M. Bacal, P. Berlemont, and F. Hillion, Phys. Rev. A **41**, 3307 (1990).
[5] L. Friedland, C. I. Ciubotariu, and M. Bacal, Phys. Rev. E **49**, 4353 (1994).
[6] M. Nishiura, M. Sasao, and M. Bacal, J. Appl. Phys. **83**, 2944 (1998).
[7] A. A. Ivanov, L. I. Elizarov, M. Bacal, and A. B. Sionov, Phys. Rev. E **52**, 6679 (1995).
[8] A. A. Ivanov, A. B. Sionov, C. I. Ciubotariu, and M. Bacal, Plasma Phys. Rep. **24**, 965 (1998).
[9] P. Berlemont, D. A. Skinner, and M. Bacal, Rev. Sci. Instrum. **64**, 2721 (1993).
[10] I. S. Gradshteyn and I. M. Ryzhik, in *Table of Integrals, Series and Products*, edited by A. Jeffrey (Academic, New York, 1980).